



CHORUS

This is the accepted manuscript made available via CHORUS. The article has been published as:

Accurate Determination of the Quasiparticle and Scaling Properties Surrounding the Quantum Critical Point of Disordered Three-Dimensional Dirac Semimetals

Bo Fu, Wei Zhu, Qinwei Shi, Qunxiang Li, Jinlong Yang, and Zhenyu Zhang

Phys. Rev. Lett. **118**, 146401 — Published 3 April 2017

DOI: [10.1103/PhysRevLett.118.146401](https://doi.org/10.1103/PhysRevLett.118.146401)

Accurate Determination of the Quasiparticle and Scaling Properties Surrounding the Quantum Critical Point of Disordered Three-dimensional Dirac Semimetals

Bo Fu,¹ Wei Zhu,^{2,3} Qinwei Shi,¹ Qunxiang Li,¹ Jinlong Yang,¹ and Zhenyu Zhang¹

¹*Hefei National Laboratory for Physical Sciences at the Microscale & Synergetic Innovation Center of Quantum Information and Quantum Physics, University of Science and Technology of China, Hefei, Anhui 230026, China*

²*Theoretical Division, Los Alamos National Laboratory, Los Alamos, New Mexico 87545, USA*

³*Center for Nonlinear Studies, Los Alamos National Laboratory, Los Alamos, New Mexico 87545, USA*

(Dated: February 8, 2017)

Exploiting the enabling power of the Lanczos method in momentum space, we determine accurately the quasiparticle and scaling properties of disordered three-dimensional Dirac semimetals surrounding the quantum critical point separating the semimetal and diffusive metal regimes. We unveil that the imaginary part of the quasiparticle self-energy obeys a common power law before, at, and after the quantum phase transition, but the power law is nonuniversal, whose exponent is dependent on the disorder strength. More intriguingly, whereas a common power law is also found for the real part of the self energy before and after the phase transition, a distinctly different behavior is identified at the critical point, characterized by the existence of a nonanalytic logarithmic singularity. This nonanalytical correction serves as the very basis for the unusual power law behaviors of the quasiparticles and many other physical properties surrounding the quantum critical point. Our approach also allows ready and reliable determination of the scaling properties of the correlation length and dynamical exponents. We further show that the central findings are valid for both uncorrelated and correlated disorder distributions, and should be directly comparable with future experimental observations.

PACS numbers: 73.43.Nq, 71.55.-i, 71.23.-k

Investigation of quantum criticality has been an important paradigm in condensed matter physics. The recent discoveries of different classes of topological materials, such as topological insulators[1–3] and Dirac or Weyl semimetals[4–8], have drastically enriched the realm of possible quantum phase transitions. In this endeavor of fundamental importance, particular attention has been paid to the effects of various physically realistic disorder, as multiple scattering of electrons from such imperfection centers may alter the quasiparticle properties of the electrons, and thereby could cause qualitative variations in the global topological properties of the whole systems. Representative examples include those from a trivial Anderson insulator to a topological Anderson insulator[9–11], from a Weyl semimetal to a quantum anomalous Hall state[12], from the quantum anomalous Hall state to an Anderson insulator[13], and from a three-dimensional (3D) Weyl or Dirac semimetal to a diffusive metal[14, 15]. A deeper microscopic understanding of the quasiparticle characteristics surrounding each type of the topological quantum phase transitions is a necessary first step towards potential technological applications of such new states of matter.

Among the different topological quantum phase transitions (QPT), that from a 3D Dirac semimetal to a diffusive metal induced by disorder has gained intensive attention over the years[14, 15]. In retrospect, this type of QPT was already investigated three decades ago in Fradkin’s pair of classic papers[16, 17]. The renewed interest has been stimulated by the latest advances in materials

realization of 3D Dirac semimetal[18–20]. Various important aspects of the transitions have been revealed based on the perturbative renormalization group (RG) analytical approaches[21–23] or numerical simulations of various physical properties surrounding the quantum critical point (QCP)[14, 15, 24, 25]. However, the disorder effects on the quasiparticle behaviors, from which many other physical observables can be derived, remain to be fully explored. Early attempts to obtain the self-energies of the quasiparticles invoked the self-consistent Born approximation[26, 27], which naturally breaks down because of its ignorance of multiple scattering events even for strong disorder[26, 28]. On a deeper and more subtle level, for such (2D or 3D) Dirac systems, the low-energy quasiparticle properties can be significantly renormalized by disorder scattering from the whole energy band[15, 29], thereby demanding highly nontrivial analytical or numerical approaches in their full and reliable determination.

In this Letter, we determine accurately the quasiparticle and scaling properties of disordered 3D Dirac semimetals surrounding the QCP separating the Dirac semimetal (DSM) and diffusive metal (DM) regimes, with all higher orders of disorder scatterings fully treated. The enabling computational approach is the Lanczos method in momentum (or k) space[30, 31]. Our simulations clearly reveal that the imaginary part of the quasiparticle self-energy obeys a common power law before, at, and after the quantum phase transition, but the power law is nonuniversal, whose exponent is dependent on the

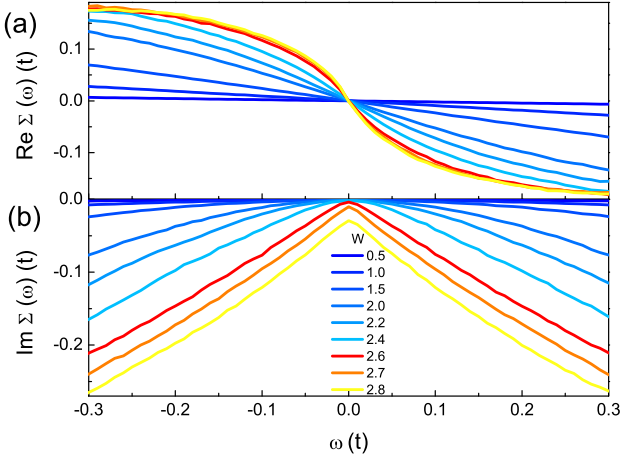


FIG. 1: (Color online). (a) Real part and (b) imaginary part of self-energy as a function of energy for different disorder strength ($0.5 \leq W \leq 2.8$). The real part of self-energy function $\text{Re}\Sigma(\omega)$ gradually deviates from linearity on the approach to the QCP. While $\text{Im}\Sigma(\omega)$ is quadratic for weak disorder, becoming linear at the QCP, and acquires a finite value $\text{Im}\Sigma(0)$ on the DM-side.

disorder strength W . More intriguingly, whereas a common power law is also found for the real part of the self energy before and after the phase transition, a distinctly different behavior is identified at the QCP, characterised by the existence of a nonanalytic logarithmic singularity. This nonanalytical correction serves as the very basis for the unusual power law behaviors of the quasiparticles and many other physical properties surrounding the QCP. The present approach also allows ready and reliable determination of the scaling properties of the correlation length and dynamical exponents. We further show that the central findings are valid for both uncorrelated and correlated disorder distributions, and should be directly comparable with future experimental observations.

Here we note that the Lanczos method in momentum space has been employed in our earlier studies of disorder effects in the specific 2D Dirac systems of graphene[30, 31]. Nevertheless, in these 2D systems, there is no such a semimetal to diffusive metal phase transition, as the disorder in graphene is perturbatively relevant for any infinitesimal or stronger disorder (namely, these is no critical disorder strength). In stark contrast, the present study focuses on 3D Dirac systems that harbor the existence of quantum phase transition from the semimetal to diffusive metal regime at the critical disorder strength, making the present study qualitatively and quantitatively beyond the earlier studies.

To start, we consider the Dirac Hamiltonian on a cubic lattice with periodic boundary conditions [32]:

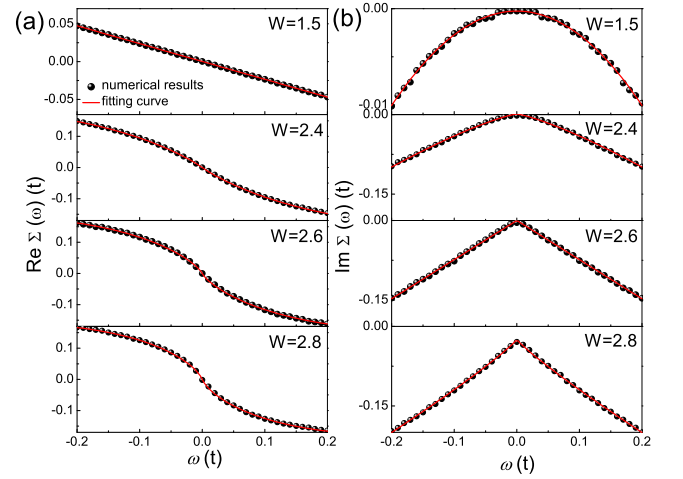


FIG. 2: (Color online). (a) The solid black circles are our numerical results of the real part of self-energy for disorder strength $W = 1.5, 2.4, 2.6, 2.8t$. The red lines are the fitting curves of Eq.(3). At the QCP ($W = 2.6t$), the fitting parameters are $2\Delta/\pi = 0.49$ and $\omega_c = 1.05$. (b) The solid black circles are the numerical results of the imaginary part of self-energy for same disorder strength. The red lines are the corresponding power law (2) fitting curves.

$$\begin{aligned}
 H &= H_0 + V \\
 &= \sum_{\mathbf{r}, \hat{\mu}} (|\mathbf{r} + e_{\hat{\mu}}\rangle \frac{it\alpha_{\hat{\mu}}}{2} \langle \mathbf{r} | + H.c.) + \sum_{\mathbf{r}} |\mathbf{r}\rangle V(\mathbf{r}) I \langle \mathbf{r} |, \quad (1)
 \end{aligned}$$

where $|\mathbf{r}\rangle$ is the four component Dirac spinor composed at site \mathbf{r} , $e_{\hat{\mu}}$ is a unit vector along the $\hat{\mu}$ direction, I represents the 4×4 identity matrix and $\alpha_{\hat{\mu}}$ are 4×4 anticommuting Dirac matrices. $V(\mathbf{r})$ represents a potential disorder distributed uniformly and independently between $[-W/2, W/2]$. In the following calculations, the hopping parameter (t) and the lattice spacing (a) is set to $t = a = 1$ for simplicity.

We use the well developed Lanczos recursive method to compute the retarded self-energy (Σ)[30, 31]. In order to be free from the the finite size errors, we adopt a large lattice containing millions of sites (300^3). Moreover, a small artificial cut-off $\eta = 0.001$ is used to simulate the infinitesimal imaginary energy in our simulations.

Before detailed discussion, we would like to give several remarks. First, the self-energy in general depends on energy (ω) and wave vector (\mathbf{k}). However, our simulation shows that the self-energy is only dependent on the energy (ω) even above the critical disorder strength. This behavior indicates that the anomalous dimension of the Dirac field vanishes. This result is consistent with one-loop renormalization group calculation[22, 23], note that our simulation is exact. Second, real parts of self energy function $\text{Re}\Sigma(\omega)$ reflect how the quasiparticle dispersion relation and the values of quasiparticle

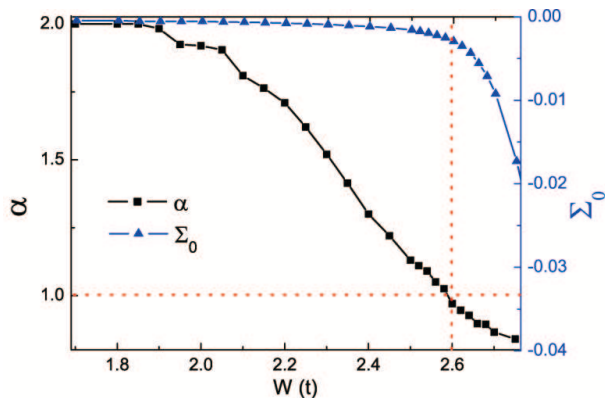


FIG. 3: (Color online). The fitting parameters Σ_0 (the blue triangles) and α (the black squares) as a function of the disorder strength. The vertical dotted (red) line denotes the critical disorder strength W_c . The horizontal dotted (red) line signifies $\alpha = 1$. The disorder strength is measured in the units of t .

residue are modified by the quantum interference arising from coherent multiply scattering. Thus, the finding of the fitting functions for the nonlinearity of $\text{Re}\Sigma(\omega)$ is very important to understand the quasiparticle behaviors around the QCP. However, the direct guess of the fitting function is quite difficult. Third, the quasiparticle residue Z_k defined as $Z_k = \frac{1}{1 - \partial_\omega \text{Re}\Sigma(\omega)}|_{\omega=E_k}$ can be used to measure the disorder effect on the quasiparticle behaviors where the quasiparticle dispersion E_k is the roots of $\omega - \hbar v_f k - \text{Re}\Sigma(\omega) = 0$. The group velocity $v_g(k)$ is given by $v_g(k) = \frac{1}{\hbar} \frac{\partial E_k}{\partial k} = Z_k v_f$. Thus, the quasiparticle residue Z_k and the group velocity v_g show the same scaling behavior around the QCP[25]. And to describe the decay time of quasiparticle, the elastic mean free time is defined as $\tau_k = \frac{\hbar}{-2Z_k \text{Im}\Sigma(E_k)}$ [33]. Here, v_f is the bare group velocity for clean three dimensional Dirac fermion and the Planck constant \hbar is set to 1.

Figure 1 plots the real part (a) and imaginary part (b) of self-energy as a function of energy for different disorder strengths. As shown, the self-energy has distinct structures as the disorder strength increases. The real part of self-energy function in the DSM phase gradually deviates from linear behavior in the vicinity of the QCP and it becomes absolutely nonlinear in DM phase. Let us focus on the imaginary part $\text{Im}\Sigma(\omega)$ firstly, we find that it remains a quadratic function of low energies in the weak disorder regime. However, the quadratical behavior changes as the disorder strength increases. Especially at the critical point, it becomes linear dependent of the energy. Above the critical strength, a finite contribution to $\text{Im}\Sigma(\omega)$ at zero energy is observed. Therefore, those observations suggest us to use a general power law expression as following to fit our numerical results:

$$\text{Im}\Sigma(\omega) = \Sigma_0 - \Delta|\omega|^\alpha. \quad (2)$$

We find the fitting is excellent as shown in Fig.2(b). Moreover, we can obtain the fitting function of $\text{Re}\Sigma(\omega)$ via the Kramers-Kronig relation [34]:

$$\text{Re}\Sigma(\omega) = \begin{cases} C\omega, & (\alpha = 2) \\ C\omega + D\text{sgn}(\omega)|\omega|^\alpha, & (1 < \alpha < 2) \\ -\frac{2\Delta}{\pi}\omega \ln\left|\frac{\omega_c}{\omega}\right|, & (\alpha = 1) \\ D\text{sgn}(\omega)|\omega|^\alpha + C\omega, & (0 < \alpha < 1) \end{cases} \quad (3)$$

where $\text{sgn}(\omega)$ is the signum function, $C = -\frac{2\omega_c^{\alpha-1}}{\pi(\alpha-1)}\Delta$ and $D = -\tan(\frac{\pi}{2}\alpha)\Delta$ are constants determined by Δ and α . Note that they are independent of Σ_0 . Fig. 2(a) shows that the fitting is also quite well as expected since they should obey the Kramers-Kronig relation. Eqs.(2) and (3) combined with our numerical calculated exponent (α) are the central results of this work.

Note that the nonanalytic corrections significantly renormalize the quasiparticle properties surrounding the QCP, making the quasiparticle spectral function at the QCP to be much broader, carrying substantially more weight in the wings than that of a normal Fermi liquid (see Supplemental Material Section I). Meanwhile, the nonanalytic correction also leads to the unusual behaviors of the physical observables. As an example, the dc conductivity shows an unusual temperature-dependent behavior near the QCP (See Supplemental Material Section II). It should be pointed out again that it is impossible to obtain this nonanalytical correction by using perturbative theory or self-consistent calculations[27], since this kind of nonanalytic correction originates from multiple scattering events.

As shown in Fig. 3, Σ_0 has a sufficient small value which equals to η ($W < 2.4$) in the DSM phase. This indicates that the rare region contribution [35–37] to the density of states at zero energy $\rho(0)$ ($\propto \Sigma_0$) should be quite small ($\ll \eta$)[38] if it exists. Very close to the critical point ($2.4 < W < 2.65$), Σ_0 increases smoothly but of the same order of magnitude as η . Thus, within the accuracy of our calculations, it is possible there is no finite contribution to Σ_0 arising from disorder scattering before the QCP since this smooth contribution to $\rho(0)$ maybe arise from the finite size effect owing to the correlation length exceeds the system size. After the QCP, Σ_0 grows rapidly when the disorder further increases (i.e. $W > 2.65$). In this situation, the DSM phase is driven into the DM phase by disorder effect.

Fortunately, note that $\text{Re}\Sigma$ is independent of Σ_0 . As we approach the QCP from the semimetal side, we can determine the critical point by the condition of the vanishing of the group velocity v_g at Dirac point. As shown in Fig.3, we find that in the DSM phase the the power law exponent (black squares) remains to be $\alpha \approx 2$ for weak disorder ($W < 1.9$), and then reduces continuously from

$\alpha \approx 2$ to 1 as the disorder strength increases towards the QCP ($1.9 < W < 2.6$). For $W > W_c$ ($W_c = 2.6$), α is reduced to less than 1. Notice that $\alpha = 1$ ($W = W_c$) corresponds to $v_g(0) = 0$ because the quasiparticle residue logarithmically vanishes in this situation, plotted as the horizontal dotted (red) line in Fig. 3. Combined these results, we obtain the critical disorder $W_c = 2.6t$ shown as the vertical dotted (red) line in Fig. 3, which agrees well with the predicted value ($W_c = 2.55 \pm 0.05$) in Ref.[25].

We then discuss how the low-energy quasiparticle behaviors change crossing the phase transition (see Table I). For weak disorder regime ($W < 1.9$), since the linear-dispersion relation is still maintained (shown as the green lines in Fig. 4(a)), we have $\alpha = 2$, the quasiparticle residue $Z_k \propto 1/(1-C)$, and the elastic mean free time $\tau_k \propto E_k^{-2}$. In the intermediate regime ($1.9 < W < W_c$), the exponent α gradually reduces, leading to the modifications of Z_k and τ_k accordingly, as shown in quasiparticle dispersion plotted as the light green lines in Fig.4(a). Remarkably, at the QCP ($W = W_c$), it is found $Z_k \propto (\ln|\omega_c/E_k|)^{-1}$ arising from nonanalytic contribution to the real part of self-energy. Thus, Z_k vanishes logarithmically as $E_k \rightarrow 0$ and $v_g(k) \rightarrow 0$, as labeled with the red line in Fig. 4(a). At the same time, τ_k behaves as $\tau_k \propto E_k^{-1} \ln|\omega_c/E_k|$ in the limit $E_k \rightarrow 0$. In the DM-phase ($W > 2.6$), the disorder is a relevant perturbation and the system displays "non-Fermi liquid" behavior with power-law energy dependence of the quasiparticle residue $Z_k \propto E_k^{1-\alpha}$, removing all remnant characters of the quasiparticle. In this regime, $v_g(k)$ goes to zero as a power law $v_g(k) \propto E_k^{1-\alpha}$ in the limit $E_k \rightarrow 0$, as shown in Fig.4(a) with the blue lines. One also finds the lifetime $\tau_k \propto Z_k^{-1} \propto E_k^{\alpha-1} \ll E_k^{-1}$. Both Z_k and τ_k exhibit quite different behavior compared with the one-loop renormalization group predictions (See Supplemental Material Section I).

Next we further discuss the critical behavior near QCP. We define the the dimensionless disorder strength parameter $\delta = |W - W_c|/W_c$ for the following discussion. Near the QCP, the spatial length scale ξ_l diverges as $\xi_l \sim \delta^{-\nu}$ and the temporal correlation length ξ_t can be measured as $\xi_t \sim \xi_l^z \propto \delta^{-\nu z}$, where the critical exponents ν and z characterize the correlations in space and time, respectively. In the language of dimensional analysis by assuming that a quantity of dimension (length $^{-D}$) is proportional to ξ_l^{-D} and of dimension time $\propto \xi_t$ or energy $\propto \xi_t^{-1}$ near the critical point, the quasiparticle disper-

TABLE I: Results of the elastic mean free time τ_k and the quasiparticle residue Z_k behaves as E_k in low energy limit for four different regimes.

	$W \leq 1.9$	$1.9 < W < W_c$	$W = W_c$	$W > W_c$
$\tau_k \propto$	E_k^{-2}	$ E_k ^{-\alpha}$	$ E_k ^{-1} \ln \omega_c/E_k $	$ E_k ^{\alpha-1}$
$Z_k \propto$	$\frac{1}{1-C}$	$\frac{1}{1-C-\alpha D E_k ^{\alpha-1}}$	$(\ln \omega_c/E_k)^{-1}$	$ E_k ^{1-\alpha}$

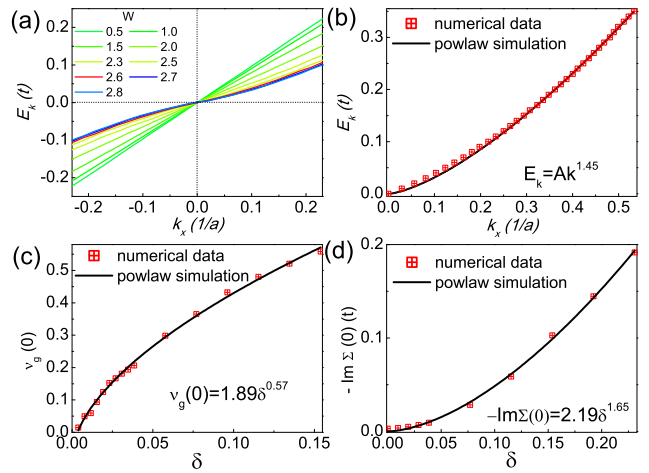


FIG. 4: (Color online). (a) The quasi-particle dispersion for different disorder strength ($0.5 \leq W \leq 2.8$). (b) The quasi-particle dispersion at the QCP (the red squares) and its power law fit (the black line) $E_k = Ak^z$ with $z = 1.45 \pm 0.05$. (c) The renormalized velocity at the Dirac point (the red squares) in DSM phase as a function of the dimensionless disorder strength $\delta = |W - W_c|/W_c$ and its power law fit (the black line) with the exponent of 0.57. (d) $-\text{Im}\Sigma(0)$ (the red squares) in DM phase as a function of δ and the power law fit (the black line) with an exponent of 1.65.

sion $E_k \sim \xi_t^{-1} \sim \xi_l^{-z} \propto k^z$ [39] and the group velocity $v_g(0) \sim \xi_l/\xi_t \propto \delta^{(z-1)\nu}$ [14]. Hence, we use the power-law form ($E_k = Ak^z$) fitting of the quasi-particle dispersion at the QCP to determine z . As shown in Fig. 4(b), the power-law fitting of E_k yields a value of $z = 1.45 \pm 0.05$ [40]. To determine the exponent ν , here we propose a method to obtain the critical exponent ν from the critical behavior of the group velocity at Dirac point $v_g(0) = v_f/(1-C)$ by the fitting parameter of Eq.(3). As shown in Fig. 4(c) by fitting the data of the vanishing velocity on the DSM side towards the critical point ($\delta = 0$) to $v_g(0) \sim \delta^{(z-1)\nu}$, we find $\nu_{DSM} = 1.14 \pm 0.10$. In DM phase, since the group velocity keeps vanishing at the Dirac point, we have to use $\rho(0) \sim -\text{Im}\Sigma(0) \sim \delta^{(3-z)\nu}$ following the previous studies[14, 24, 25]. By fitting the data we find $\nu_{DM} = 1.06 \pm 0.16$ as shown in Fig. 4(d). Our simulations about the critical exponents are consistent with the values obtained to the one-loop renormalization group calculation[21–23].

So far, we have limited our discussions to situations with uncorrelated Anderson disorder. To enable more direct comparisons with future physically realistic measurements, we expand our model studies to systems with correlated disorder, as described by random yet varyingly correlated Gaussian potentials. We find that, whereas the specific location of the QCP sensitively depends on both the strength and degree of correlation of the disorder, the very existence of the quantum phase transition and scaling properties of the critical exponents are in-

sensitive to the details of such disorder distributions (See Supplemental Material Section III). This further exploration effectively broadens the applicability of the main findings of this work.

Additionally, our calculations further show that it is not essential to reveal our main findings by fixing the Fermi level at the critical point (the Dirac point), because the novel anomalous behavior can be observed over a substantial energy (see Fig. 4) or temperature range. As a promising candidate system, we suggest Na_3Bi [41], whose Fermi surface is close to the Dirac point. By disordering it to the quantum phase transition regime, we expect that anomalous quasiparticle and unusual scaling behaviors are likely to be observed.

In summary, by using the numerically exact Lanczos method in k space, we have calculated the real and imaginary parts of the quasiparticle self-energy for disordered 3D Dirac semimetals, and then determined the nonanalytic correction to the self-energy $\Sigma(\omega)$ at or above the QCP, which leads to the unusual behaviors of the low-energy quasiparticles and other physical observables. These new and striking predictions call for direct experimental validations. Moreover, the numerical approach introduced here is transformative, and can be applied to other quantum phase transitions induced by disorder.

This work was partially supported by the State Key Research & Development Program of China (No. 2016YFA0200600), by National Key Basic Research Program (Nos. 2014CB921101), by the NSFC (Nos. 21473168 and 11634011). WZ was supported by US DOE through Los Alamos National Laboratory LDRD program (No. DE-AC52-06NA25396) and PRD program (No. DR-20170664PRD1). Computational resources have been provided by CAS, Shanghai and USTC Supercomputer Centers.

[1] B. A. Bernevig, T. L. Hughes, and S.-C. Zhang, *Science* **314**, 1757 (2006).
 [2] M. Z. Hasan and C. L. Kane, *Rev. Mod. Phys.* **82**, 3045 (2010).
 [3] X.-L. Qi and S.-C. Zhang, *Rev. Mod. Phys.* **83**, 1057 (2011).
 [4] X. Wan, A. M. Turner, A. Vishwanath, and S. Y. Savrasov, *Phys. Rev. B* **83**, 205101 (2011).
 [5] K. Y. Yang, Y. M. Lu, and Y. Ran, *Phys. Rev. B* **84**, 075129 (2011).
 [6] G. Xu, H. Weng, Z. Wang, X. Dai, and Z. Fang, *Phys. Rev. Lett.* **107**, 186806 (2011).
 [7] S. M. Young, S. Zaheer, J. C. Y. Teo, C. L. Kane, E. J. Mele, and A. M. Rappe, *Phys. Rev. Lett.* **108**, 140405 (2012).
 [8] B. -J. Yang, M. S. Bahramy, R. Arita, H. Isobe, E.-G. Moon, and N. Nagaosa, *Phys. Rev. Lett.* **110**, 086402 (2013).
 [9] J. Li, R.-L. Chu, J. K. Jain, and S.-Q. Shen, *Phys. Rev.*

Lett. **102**, 136806 (2009).
 [10] C. W. Groth, M. Wimmer, A. R. Akhmerov, J. Tworzydło, and C. W. J. Beenakker, *Phys. Rev. Lett.* **103**, 196805 (2009).
 [11] K. Kobayashi, T. Ohtsuki, and K.-I. Imura, *Phys. Rev. Lett.* **110**, 236803 (2013).
 [12] C.-Z. Chen, J. Song, H. Jiang, Q.-F. Sun, Z. Wang, and X. C. Xie, *Phys. Rev. Lett.* **115**, 246603 (2015).
 [13] Z. Qiao, Y. Han, L. Zhang, K. Wang, X. Deng, H. Jiang, S. A. Yang, J. Wang, and Q. Niu, *Phys. Rev. Lett.* **117**, 056802 (2016).
 [14] K. Kobayashi, T. Ohtsuki, K.-I. Imura, and I. F. Herbut, *Phys. Rev. Lett.* **112**, 016402 (2014).
 [15] S. V. Syzranov, L. Radzihovsky, and V. Gurarie, *Phys. Rev. Lett.* **114**, 166601 (2015).
 [16] E. Fradkin, *Phys. Rev. B* **33**, 3257 (1986).
 [17] E. Fradkin, *Phys. Rev. B* **33**, 3263 (1986).
 [18] Z. Liu, J. Jiang, B. Zhou, Z. Wang, Y. Zhang, H. Weng, D. Prabhakaran, S. Mo, H. Peng, P. Dudin, T. Kim, M. Hoesch, Z. Fang, X. Dai, Z. X. Shen, D. L. Feng, Z. Hussain, and Y. L. Chen, *Nat. Mater.* **13**, 677 (2014).
 [19] S. Borisenko, Q. Gibson, D. Evtushinsky, V. Zabolotnyy, B. Buchner, and R. J. Cava, *Phys. Rev. Lett.* **113**, 027603 (2014).
 [20] M. Neupane, S.-Y. Xu, R. Sankar, N. Alidoust, G. Bian, C. Liu, I. Belopolski, T.-R. Chang, H.-T. Jeng, H. Lin, A. Bansil, F. C. Chou, and M. Z. Hasan, *Nat. Commun.* **5**, 3786 (2014).
 [21] P. Goswami, and S. Chakravarty, *Phys. Rev. Lett.* **107**, 196803 (2011).
 [22] B. Roy and S. Das Sarma, *Phys. Rev. B* **90**, 241112(R) (2014).
 [23] S. V. Syzranov, P. M. Ostrovsky, V. Gurarie, and L. Radzihovsky, *Phys. Rev. B* **93**, 155113 (2016).
 [24] S. Bera, J. D. Sau, and B. Roy, *Phys. Rev. B* **93**, 201302 (2016).
 [25] J. H. Pixley, P. Goswami, and S. Das Sarma, *Phys. Rev. B* **93**, 085103 (2016).
 [26] B. Sbierski, G. Pohl, E. J. Bergholtz, and P. W. Brouwer, *Phys. Rev. Lett.* **113**, 026602 (2014).
 [27] Y. Ominato, and M. Koshino, *Phys. Rev. B* **89**, 054202 (2014).
 [28] H. Shapourian and T. L. Hughes, *Phys. Rev. B* **93**, 075108 (2016).
 [29] I. L. Aleiner, and K. B. Efetov, *Phys. Rev. Lett.* **97**, 236801 (2006).
 [30] W. Zhu, Q. W. Shi, X. R. Wang, X. P. Wang, J. L. Yang, J. Chen, and J. G. Hou, *Phys. Rev. B* **82**, 153405 (2010).
 [31] W. Zhu, W. Li, Q. W. Shi, X. R. Wang, X. P. Wang, J. L. Yang, and J. G. Hou, *Phys. Rev. B* **85**, 073407 (2012).
 [32] J. H. Pixley, P. Goswami, and S. Das Sarma, *Phys. Rev. Lett.* **115**, 076601 (2015).
 [33] G. D. Mahan, *Many Particle Physics* (Kluwer Academic/Plenum Publisher, New York, 2000).
 [34] The general Kramers-Kronig relationship is

$$\text{Re}\Sigma(\omega) = \frac{1}{\pi} P \int_{-\omega_c}^{\omega_c} d\omega' \frac{\text{Im}\Sigma(\omega')}{\omega' - \omega}, \quad (4)$$
 where P signifies the Cauchy principal value of the integral, ω_c is the upper energy cutoff and has the order of the magnitude of the band width ≈ 1 .
 [35] R. Nandkishore, D. A. Huse, and S. L. Sondhi, *Phys. Rev. B* **89**, 245110 (2014).

- [36] S. V. Syzranov, V. Gurarie, and L. Radzihovsky, Phys. Rev. B **91**, 035133 (2015).
- [37] J. H. Pixley, D. A. Huse, and S. DasSarma, Phys. Rev. X **6**, 021042 (2016).
- [38] In all cases discussed below, we ignore the rare region effect on the elastic time in the DSM side by setting $\text{Im}\Sigma(0)$ to zero. If considering this nonperturbative effect, a direct extension of the present results can be obtained just by taking a small finite value of $\text{Im}\Sigma(0)$ into account see ref.39.
- [39] A. W. W. Ludwig, M. P. A. Fisher, R. Shankar, and G. Grinstein, Phys. Rev. B **50**, 7526 (1994).
- [40] The error is estimated by considering the uncertainty of the range over which the numerical results are fitted to extract the power-law dependence. We do not fit the numerical data sufficiently close to the Dirac point, as that the correlation length exceeds the system size suffering from severe finite-size effects.
- [41] Z. K. Liu, B. Zhou, Y. Zhang, Z. J. Wang, H. M. Weng, D. Prabhakaran, S.-K. Mo, Z. X. Shen, Z. Fang, X. Dai, Z. Hussain, and Y. L. Chen, Science **343**, 864 (2014).